● RESEARCH ARTICLE

No DCX-positive neurogenesis in the cerebral cortex of the adult primate
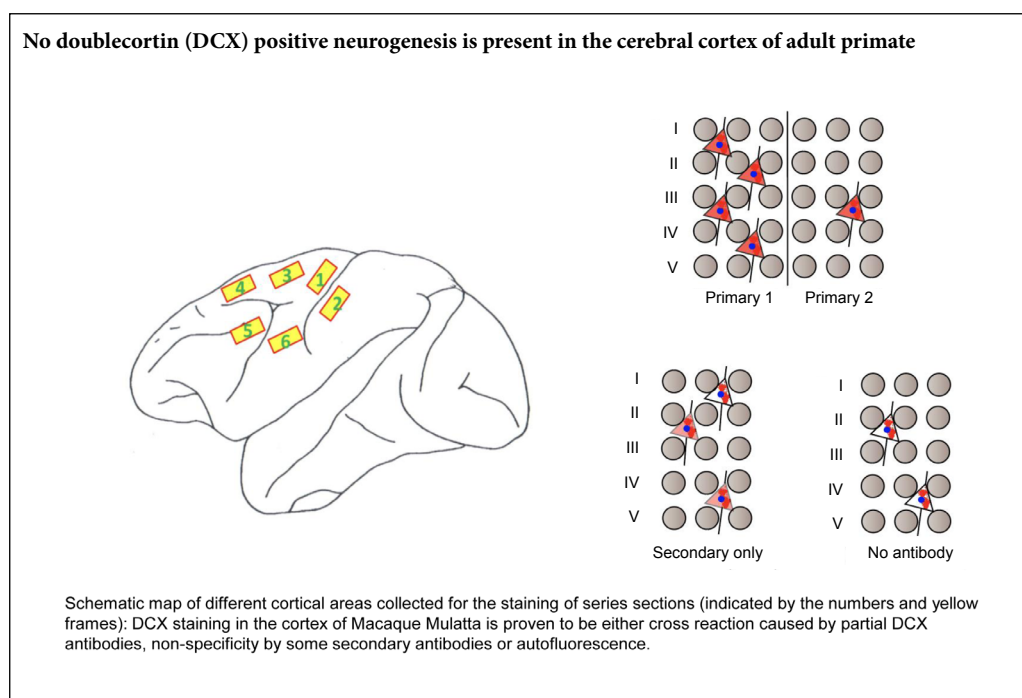
Ruo-Xu Liu[1, *], Jie Ma[1], Bin Wang[1], Tian Tian[2], Ning Guo[1], Shao-Jun Liu[1, *]

1 Institute of Military Cognition and Brain Sciences, Beijing, China
2 Department of Pharmacy, Medical College, Huanghe S&T University, Zhengzhou, Henan Province, China

Graphical Abstract

No doublecortin (DCX) positive neurogenesis is present in the cerebral cortex of adult primate

Schematic map of different cortical areas collected for the staining of series sections (indicated by the numbers and yellow frames): DCX staining in the cortex of Macaque Mulatta is proven to be either cross reaction caused by partial DCX antibodies, non-specificity by some secondary antibodies or autofluorescence.

Abstract

Whether endogenous neurogenesis occurs in the adult cortex remains controversial. An increasing number of reports suggest that doublecortin (DCX)-positive neurogenesis persists in the adult primate cortex, attracting enormous attention worldwide. In this study, different DCX antibodies were used together with NeuN antibodies in immunohistochemistry and western blot assays using adjacent cortical sections from adult monkeys. Antibody adsorption, antigen binding, primary antibody omission and antibody-free experiments were used to assess specificity of the signals. We found either strong fluorescent signals, medium-weak intensity signals in some cells, weak signals in a few perikarya or near complete lack of labeling in adjacent cortical sections incubated with the various DCX antibodies. The putative DCX-positive cells in the cortex were also positive for NeuN, a specific marker of mature neurons. However, further experiments showed that most of these signals were either the result of antibody cross reactivity, the non-specificity of secondary antibodies or tissue autofluorescence. No confirmed DCX-positive cells were detected in the adult macaque cortex by immunofluorescence. Our findings show that DCX-positive neurogenesis does not occur in the cerebral cortex of adult primates, and that false-positive signals (artefacts) are caused by antibody cross reactivity and autofluorescence. The experimental protocols were approved by the Institutional Animal Care and Use Committee of the Institute of Neuroscience, Beijing, China (approval No. IACUC-AMMS-2014-501).

Key Words: *adult neurogenesis; antigen neutralization; autofluorescence; cross reaction; cross reactivity; doublecortin; neocortex; NeuN; non-specificity; primates; tissue adsorption*

Chinese Library Classification No. *R453; R363; R364*

Introduction

Because of the importance of the neocortex and its intricate connections, endogenous neurogenesis in the cerebral cortex of adult primates has attracted enormous attention worldwide for the treatment of neurological disease and aging. Previous studies using BrdU labeling reported endogenous neurogenesis in the cerebral cortex of adult primates (Gould et al., 1999; He et al., 2019). However, Kornack and Rakic showed that the so-called endogenous neurogenesis in the adult primate cortex was caused by the spatial overlap of BrdU-positive nuclei and the perikarya of NeuN-positive neurons, leading to the wrong conclusion (Kornack and Rakic, 2001; Rakic, 2002). Numerous reports have subsequently described the presence or absence of endogenous neurogenesis in the cerebral cortex of nonhuman primates by doublecortin (DCX) immunolabeling (Qin et al., 2000; Fung et al., 2011; Nacher and Bonfanti, 2015).

DCX is a microtubule and actin filament-associated protein (Dhaliwal et al., 2015; Moslehi et al., 2017; Han et al., 2018; Zhou et al., 2019). Because of its specific expression in neural precursors and newly-generated immature neurons in many brain regions of both developing and adult mammals, DCX has been used as a specific marker of neural precursors and immature neurons to evaluate potential endogenous neurogenesis in the adult brain (Francis et al., 1999; Gleeson et al., 1999; Brown et al., 2003; Schaar et al., 2004; Tsukada et al., 2005; Fournier et al., 2018; Shahsavani et al., 2018). Using DCX immunolabeling, a few studies reported that DCX-positive immature neurons are not detectable in the cerebral cortex of adult primates (Bonfanti and Nacher, 2012; Stanton et al., 2015). However, the overwhelming majority of studies have reported that DCX-positive cells persist in the neocortex of adult primates (Liu et al., 2008, 2018; Cai et al., 2009; Zhang et al., 2009; Bloch et al., 2011; Stanton et al., 2015; Fasemore et al., 2018), although some with some uncertainty (Feliciano et al., 2015; Lipp and Bonfanti, 2016). Along with the further increase in these studies (Abrous et al., 2005), DCX-positive neurogenesis in the brain has again aroused the attention of the public. However, more recently, there have been contradictory findings on the presence of endogenous DCX-positive neurogenesis in the adult human hippocampus (Ehninger and Kempermann, 2008; Lipp and Bonfanti, 2016; Boldrini et al., 2018; Kempermann et al., 2018; Tobin et al., 2019). Based on DCX labeling of sheep brain sections, Piumatti et al. (2018) proposed a new form of brain structural plasticity, as they found that the DCX-expressing cells are generated prenatally and remain in a state of immaturity for long periods. However, it is unclear why and how these "immature neurons" exhibiting a morphology and markers typical of mature neurons have yet differentiated into mature neurons in the adult cortex.

It remains poorly understood why there are contradictory findings on endogenous neurogenesis in the adult primate cortex by DCX antibody labeling. To our knowledge, no one has yet raised concerns over the specificity of DCX antibodies used in these published studies. Therefore, in the present study, we investigated whether some of these inconsistencies are caused by non-specific immunolabeling.

Materials and Methods

Animals

Six adult rhesus macaques (Macaca mulatta), 9–10-years-old, were provided by Beijing Primas Biotech Co., Ltd., Beijing, China (SCXK(Jing) 2018-0001). All animals were maintained on a 12-hour day/night cycle with lights on at 06:00, at 24°C with 30–50% relative humidity. The experimental protocols were approved by the Institutional Animal Care and Use Committee of the Institute of Neuroscience, Beijing, China (approval No. IACUC-AMMS-2014-501).

Immunofluorescence labeling

Under deep anesthesia, the macaques were perfused with saline solution and then 4% formaldehyde in ice-cold phosphate buffer. The different regions of the neocortex (**Additional Figure 1**) and subventricular zone (SVZ) were dissected and post-fixed for 4 hours in 4% formaldehyde, and then transferred to 20% sucrose solution overnight at 4°C. Frozen sections were cut at 20-μm-thickness, 28 sections/series, and incubated in phosphate-buffered saline (PBS) containing 4% donkey serum, 0.3% bovine serum albumin and 0.3% Triton at room temperature for 2 hours. These sections were then incubated with different DCX antibodies, including Ab18723-1 (1:1000), Ab18723-2 (1:2000), 4064 (1:400; Cell Signaling Technology, Danvers, MA, USA), Sc-8066 (1:100) and Sc-271390 (1:100) (**Additional Table 1**), for 24 hours at 4°C, followed by three washes in PBS for 10 minutes each. Afterwards, the sections were incubated with the corresponding Alexa Fluor-conjugated secondary antibodies (unadsorbed or adsorbed) for 2 hours, washed three times in PBS, stained with Hoechst 33258 (Lot No, B28838; Sigma-Aldrich, St. Louis, MO, USA) or DAPI (Lot No, D9642, 1:1000; Sigma-Aldrich) for 10 minutes, and mounted using F4680 Fluoromount Aqueous mounting medium (Lot# SLBQ2436V, Sigma-Aldrich) to prevent fluorescence quenching.

Adsorption of antibodies with tissues and antigens

Tissue adsorption with DCX antibodies was performed using adult rat cortex sections. Adult rats were first perfused with saline solution and then 4% formaldehyde in ice-cold phosphate buffer for 2 hours. The brains were then removed and post-fixed in the same solution for 4 hours, and then transferred to 20% sucrose solution overnight at 4°C. The cerebral cortices were dissected under an anatomical microscope to eliminate subcortical tissue. After 20-μm sectioning, horizontal or coronal, the frozen cortical sections were permeabilized in 1% Triton X-100 for 1 hour, and then incubated with the antibody working solutions for 6 hours. Cortical sections that had been incubated with the primary antibodies were labeled with secondary antibody and examined under the fluorescence microscope. The whole process (**Additional Figure 2**) was repeated once more until no immunofluorescence labeling was present on the sections. Frozen cortex and SVZ sections of the rhesus monkey were stained with several combinations of primary and secondary

antibodies with or without rat brain tissue adsorption.

Antigen adsorption experiments were conducted with antibodies ab18723-1 and ab18723-2 (Abcam, Cambridge, MA, USA). Human DCX peptide (Lot: GR3178653-2, ab19804, Abcam, working concentration 0.5 ng/μL) was applied to an appropriate concentration (less than 2 ng/μL) of antibodies at room temperature for 4 hours. The adsorbed and unadsorbed antibodies were then used to label the adjacent sections of the cerebral cortex of the adult macaque for 12 hours, followed by the corresponding fluorescein-conjugated secondary antibodies (ab150072 or A11036).

DCX primary antibody omission experiment
To test for non-specific labeling by secondary antibodies, nine different secondary antibodies (**Additional Table 1**) were pre-adsorbed with the rat cortex sections, as described above. The adjacent sections of the cerebral cortex of the adult macaque were incubated with NeuN antibody (mouse monoclonal NeuN antibody ab104224; working dilution 1:500; Abcam) and the corresponding secondary combinations, Ab181289 (1:200, green, donkey anti-mouse IgG conjugated with Alexa Fluor 488; Abcam) and one of five unrelated secondary antibodies (red), Ab150131 (1:200, donkey anti-goat IgG H&L (Alexa Fluor 647)), Ab150112 (1:200, donkey anti-mouse IgG H&L (Alexa Fluor 594)), Ab150072 (1:200, donkey F(ab')2 anti-rabbit IgG H&L (Alexa Fluor 594)), A11031 (1:500, goat anti-mouse IgG (H+L) highly cross-adsorped secondary antibody (Alexa Fluor 568)) or A11036 (1:500, goat anti-rabbit IgG (H+L) highly cross-adsorped secondary antibody (Alexa Fluor 568)), that had been adsorbed or unadsorbed with rat cortex sections. Alternatively, the adjacent cortex sections were labeled with NeuN antibody (ab104224, Abcam), and then with the corresponding adsorbed or unadsorbed secondary combinations (Ab150112, donkey anti-mouse IgG H&L (Alexa Fluor 594; red)) and either Ab181289 (1:200, donkey F(ab')2 anti-mouse IgG H&L (Alexa Fluor 488; green)), Ab181346 (1:200, donkey F(ab')2 anti-rabbit IgG H&L (Alexa Fluor 488)), A11029 (1:500, goat anti-mouse IgG (H+L) highly cross-adsorped secondary antibody, (Alexa Fluor 488)) or A11034 (1:500, goat anti-rabbit IgG (H+L) highly cross-adsorped secondary antibody (Alexa Fluor 488)). All the sections were mounted with an anti-quenching agent, F4680 Fluoromount Aqueous mounting medium (Lot# SLBQ2436V, Sigma-Aldrich).

Antibody-free experiments
Adjacent cryostat sections of the adult macaque cortex were mounted using F4680 Fluoromount Aqueous mounting medium (Lot# SLBQ2436V, Sigma-Aldrich) with a cover glass immediately after slicing, without any other treatment. Alternatively, the adjacent sections were incubated with the diluents without primary or secondary antibody for 4 hours, and then mounted as above.

The results were observed under a microscope (BX50; Olympus, Tokyo, Japan). Immunofluorescence images were captured on a confocal microscope (880; Zeiss, Oberkochen,

Germany). The spectral analysis of fluorescence points and the adjustments of brightness and contrast were performed using the same software. All images in the same figures were adjusted with identical contrast and brightness settings.

Data acquisition
Spectral analysis was performed with the Zeiss laser confocal microscope (880; Zeiss). The fluorescence intensity was directly assessed under a fluorescence microscope (Olympus), and the data were confirmed by spectral analysis.

Western blot assay of the adult macaque tissues
Under deep anesthesia, the skin, skull and meninges of the rhesus monkey were quickly opened, and the brain was removed under a stereomicroscope. The anterior central gyrus and the medial regions of the prefrontal cortex (cerebral gyri on both sides of the anterior central longitudinal sulcus) were removed. Subcutaneous tissues around the cortical regions were carefully removed under the anatomical microscope. The SVZ of the lateral ventricle was also separated under the operating microscope. For western blot assay, tissues from the cortex and SVZ were homogenized in lysis buffer (RIPA R0278, Sigma-Aldrich; protein inhibitor 04693159001, Roche, Hertfordshire, UK), and 25 μg of total protein was loaded on the gel. The blots were incubated with primary antibodies against DCX, 4604S (Cell Signaling Technology), sc-8066 and sc-271390 (Santa Cruz Biotechnology, Santa Cruz, CA, USA), ab18723 (Lot# GR281032-1 and GR3224908-1, Abcam; with or without tissue-adsorption) or cofilin (10960-1-AP, Proteintech, Chicago, IL, USA) at 4°C overnight, followed by incubation with the corresponding secondary antibody (HRP-conjugated, Proteintech) for 1 hour at room temperature. Membranes were exposed to enhanced chemiluminescence reagents (Beyotime, Nantong, China) and visualized using ImageQuant LAS 500 (GE, Fairfield, CT, USA).

Data analysis
Six to nine randomly selected fields were captured on a laser confocal microscope (880; Zeiss) for each slice. The number of positive cells was counted with ImageJ (Jensen, 2013) and Fiji (Schindelin et al., 2012) software packages using point picker or particle analysis (Drury et al., 2011; Vayrynen et al., 2012; Diem et al., 2015). A uniform background was acquired through shading correction (Model and Burkhardt, 2001). The percentage of DCX-positive cells was calculated as (DCX-positive cell count/neuron count) × 100.

Results
Comprehensive analysis of the distribution of DCX-positive neurons in adjacent sections of the cortex and SVZ in the adult macaque
The adjacent frozen sections were incubated with different commercial DCX antibodies and corresponding fluorescein-conjugated second antibodies (**Additional Table 1**) under the same conditions. In sections incubated with primary antibody ab18723-1 (Lot. GR281032-1; Abcam) and secondary

antibody A11036 (Thermo Fisher Scientific, Waltham, MA, USA), a large number of DCX-positive neurons with medium fluorescence intensity (86% of total cortical neurons) were observed throughout the cortex (**Table 1**).

In the adjacent sections incubated with DCX antibody ab18723-1 and secondary antibody ab150072 (Abcam), comparatively stronger fluorescence was seen in almost all neurons (98%) and their protuberances in laminae II–VI of the cortex, especially in pyramidal cells in laminae III and V (**Figure 1A, Table 1**, and **Additional Figure 3A**).

In the adjacent sections incubated with DCX antibodies ab18723-2 (Lot. GR3224908-1; Abcam) and the corresponding secondary antibody, ab150072, medium intensity fluorescence was observed in 46% of perikarya and thick protuberances in layer V of the cortex (**Figure 1A, Table 1**, and **Additional Figure 3B**).

In adjacent sections incubated with DCX antibodies ab18723-2 and secondary antibody A10036, a similar distribution of DCX-positive cells (37%), but with weaker fluorescence, was observed in the cortex.

In adjacent cortical sections incubated with DCX primary antibody 4604S (Cell Signaling Technology) and secondary antibody ab150072, weak fluorescence was visible in a few perikarya (3.5%) in layers III and V (**Figure 1A, Table 1**, and **Additional Figure 3C**).

In sections incubated with 4604S and A11036, the percentage of DCX-positive neurons was smaller (0.2%), and red fluorescent signals (appearing as granules and lumps) were much weaker in the perikarya (**Table 1**) of pyramidal cells in laminae III and V.

In sections incubated with DCX antibody sc-271390 and secondary antibody ab150112 (**Additional Table 1**), only a few cells (0.5%) with weak fluorescence signals were detected in the cortex.

In adjacent sections incubated with DCX antibody sc-271390 and A11031 (**Additional Table 1**), the contours of perikarya with very weak fluorescence (**Figure 1A, Table 1,** and **Additional Figure 3D**) were observed. In adjacent sections incubated with DCX antibody sc-8066 and corresponding secondary antibody Ab150131 (**Additional Table 1**), a similar result was found.

In the controls, strong fluorescence was found in sparse cell-like structures in the SVZ (**Table 1** and **Additional Figure 3A–D**), irrespective of the combination of primary and secondary antibodies used.

Interestingly, all DCX-positive signals, whether strong or weak, were co-localized with the neuron-specific nuclear protein NeuN, a marker of mature neurons, in the perikarya of cortical neurons (**Figure 1A** and **Additional Figure 3**), but not in the cells of the SVZ (**Additional Figure 3**). In addition, the strong fluorescent clusters and dispersed particles were also co-localized in NeuN-positive perikarya mainly in layers III and V of the cortex for all antibody combinations (**Figure 1A, B** and **Additional Figure 3**). To further charac-

Table 1 Distribution of DCX positive labeling in the cerebral cortexes of adult primates with or without tissue and antigen adsorption

		Primary antibodies/disposition/brain region									
		Abcam 18723-1 (Lot.GR281032-1)						Abcam 18723-2 (Lot.GR3224908-1)			
		Unabsorbed		Tissue absorption		Antigen absorption		Unabsorbed		Tissue absorption	
		Cortex	SVZ	Cortex	SVZ	Cortex	SVZ	Cortex	SVZ	Cortex	SVZ
Secondary antibodies	Abcam 150072 (Unabsorbed)	++++	+++++	±	++++	++	–	+++	++++	+	++++
	Abcam 150072 (Absorbed)	+++	+++++	±	++++	+	–	++	+++	±	+++
	Thermo A11036 (Unabsorbed)	+++	++++	–	++++	++	–	++	++++	±	++++
	Thermo A11036 (Absorbed)	+++	++++	–	+++	+	–	++	+++	±	++++
	Abcam 150112 (Unabsorbed)										
	Abcam 150112 (Absorbed)										
	Thermo A11031 (Unabsorbed)										
	Thermo A11031 (Absorbed)										

		Primary antibodies/disposition/brain region									
		Abcam 18723-2 (Lot.GR3224908-1)		CST-4604				SC-271390*			
		Antigen absorption		Unabsorbed		Tissue absorption		Unabsorbed		Tissue absorption	
		Cortex	SVZ	Cortex	SVZ	Cortex	SVZ	Cortex	SVZ	Cortex	SVZ
Secondary antibodies	Abcam 150072 (Unabsorbed)	++	–	+	++++	±	++++				
	Abcam 150072 (Absorbed)	+	–	±	++++	–	++++				
	Thermo A11036 (Unabsorbed)	+	–	±	++++	–	++++				
	Thermo A11036 (Absorbed)	+	–	–	++++	–	++++				
	Abcam 150112 (Unabsorbed)							±	++++	–	++++
	Abcam 150112 (Absorbed)							–	++++	–	++++
	Thermo A11031 (Unabsorbed)							±	++++	–	++++
	Thermo A11031 (Absorbed)							–	++++	–	++++

*There were no significant differences between SC-271390 and SC-8066. "+, ± and –": Fluorescence intensity from observation and spectrometric determination. "±" Indicates that the outlines of the perikarya were weakly immunolabeled or that the immunofluorescence was only slightly above background in subsequent quantitative spectroscopy examinations. DCX: Doublecortin; SVZ: subventricular zone.

terize these strong fluorescent signals, *in situ* spectral analysis of neuron perikarya was performed. When the excitation wavelength was 488 nm or 561 nm, the emission wavelengths of the strong fluorescent masses in the perikarya ranged from 500 nm or 568 nm to infrared (**Figure 1B** and **Additional Figure 3B**), which is far beyond the emission range of fluorescein-conjugated secondary antibodies (**Additional Table 1**). The broad spectrum of the emitted light is characteristic of autofluorescence.

Tissue adsorption of DCX primary antibodies
To examine the specificity of the DCX antibodies, pre-adsorption experiments were performed with the four different DCX primary antibodies and corresponding secondary antibodies (**Table 1**). The antibodies were pre-incubated with rat cortex sections. Then, adjacent cryostat sections of adult rhesus cortices were incubated with the various combinations of DCX primary antibody (Ab18723-1, Ab18723-2 and 4604 (adsorbed or unadsorbed; Cell Signaling Technology)) and Alexa Fluor-conjugated secondary antibody (adsorbed or unadsorbed). The immunofluorescence signals almost completely disappeared in the cortex, except for the fluorescence granules and clusters shown to be autofluorescence artefacts (**Figure 2A** and **Table 1**). On some adjacent sections incubated with the adsorbed DCX antibody and the unadsorbed secondary antibody, a few cells with weak fluorescence were observed (**Table 1**), which we subsequently show to be caused by non-specific binding by the secondary antibody. When incubated with the tissue-adsorbed DCX antibody sc-271390 and the corresponding tissue-adsorbed secondary antibody A11031 (Thermo Fisher Scientific; **Additional Table 1**) or ab150112, red fluorescence was undetectable (**Table 1**). The same results were obtained for the six cortical regions that were examined (**Additional Figure 1**).

As control, SVZ sections were labeled with the same primary and secondary antibodies with or without adsorption (**Figure 2B** and **Table 1**). When the spectral characteristics were compared, an overall attenuation in background signal was detected, with a rather small loss in DCX immunofluorescence intensity after pre-adsorption (**Figure 2B** and **Table 1**).

Antigen neutralization of DCX primary antibodies
Antigen neutralization experiments with DCX antibodies were carried out by incubating DCX antibodies ab18723-1 and ab18723-2 with their corresponding antigen (**Additional Table 1**). In sections treated with these antigen pre-adsorbed antibodies, most of the putative DCX immunoreactivity in the cortex decreased significantly, but remained at a moderate intensity (**Figure 3a–c** and **Table 1**). In comparison, no DCX-positive labeling was detected in the SVZ (**Figure 3d** and **Table 1**), confirming that the DCX antibody had been adsorbed completely by DCX antigen. To exclude non-specific immunolabeling caused by other factors, the pre-adsorbed secondary antibodies were matched with the antigen-neutralized DCX antibodies for staining. The intensity of the red fluorescence was further reduced, but was still significantly higher than the background fluorescence (**Figure 3e–i** and **Table 1**), indicating that partial cross-reactivity remained.

DCX primary antibody omission experiments
The fluorescence in a few cortical neurons was weak but still discernible in adjacent cortex sections incubated only with secondary antibodies ab150112, ab150131 and ab150072 (**Figure 4A**, **Additional Figure 4A** and **Additional Table 2**). When the sections were incubated with ab150112, ab150131 and ab150072 pre-adsorbed with rat cortex sections, the fluorescence signals became weaker and closer to background (**Figure 4B**, **Additional Figure 4B** and **Additional Table 2**). Spectral analysis of the fluorescence showed that the intensity of the emissions was very similar to background (**Figure 4**). When the adjacent sections were incubated with the six remaining secondary antibodies (ab181289, ab181346, A11029, A11031, A11034 and A11036), the fluorescence was weaker and barely distinguishable (**Additional Table 2**).

Primary and secondary antibody omission experiments
To further characterize the fluorescence particles and clusters in the cortical neurons, adjacent sections of the adult macaque cortex were mounted directly and immediately after slicing without any other treatment (**Figure 5A**) or only incubated in the serum diluent without any antibody (**Figure 5B**). The strongly fluorescent particles and clusters still persisted in the perikarya of the cortical neurons (**Figure 5A** and **B**). When excited at 488 nm and 561 nm, the fluorescence intensity of these scattered signals within the perikarya was much higher than that of the large masses. The former was also difficult to quench by laser during scanning and observation (**Figure 5C**).

Comparison of antibodies on western blot of the adult macaque brain
DCX antibodies from different companies or with different product or batch numbers were used for immunohistochemistry of the cortex and SVZ from six monkeys (**Figure 6A**). There was a clear band around 45 kDa in the SVZ. The same band was barely visible in the cortex when incubated with the antibodies mentioned above.

Next, we examined each antibody for specificity using hippocampus, cortex and SVZ from six monkeys, using 25 μg of total protein per lane. Apart from the presence of the 45 kDa predicted band, Ab18723-1 produced bands at 100 and 150 kDa as well. Ab18723-2 labeled bands at over 150 and 75 kDa (**Figure 6B**). These extraneous bands were not found in blots of P0 brain tissues incubated with Ab18723-1. Other antibodies did not produce extraneous bands.

Tissue pre-adsorption was used on antibodies Ab18723-1 and Ab18723-2. The latter as then used for western blot assay as described above. Bands around 45 kDa were no longer detected with either Ab18723-1 or Ab18723-2 adsorbed antibody. Extraneous bands around 150 kDa for Ab18723-1 and over 150 kDa for Ab18723-2 were attenuated but still visible (**Figure 6C**).
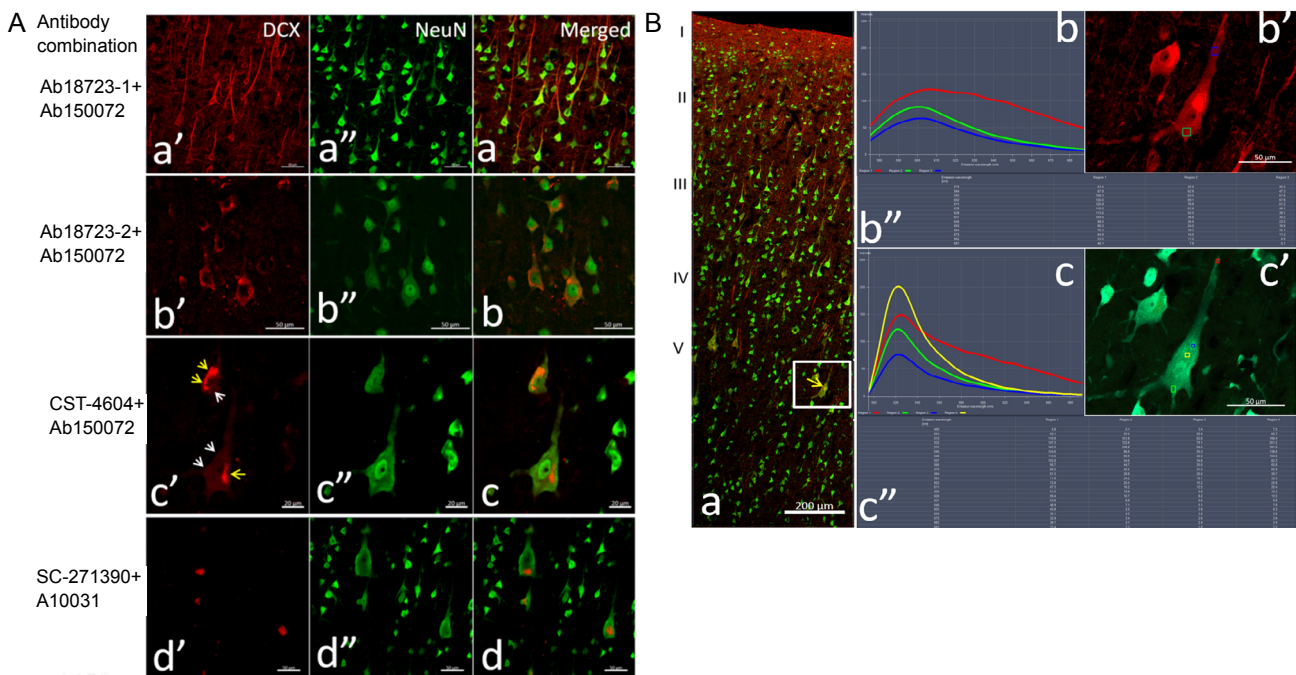
Figure 1 Distribution of DCX-positive labeling in adjacent adult monkey brain cortex sections labeled with different primary antibodies.
(A) DCX staining using different antibody combinations. Antibodies Ab18723-1, Ab18723-2, CST-4604 and SC-271390 and their corresponding fluorescein-conjugated secondaries were used on adjacent sections of the cortex. Panels a-d show brain sections stained with different antibody combinations. In each row, DCX (a'–d'), Neun (a''–d'') and their merged channels are presented sequentially. The photomicrographs are of layers III (panel a) and V (panels b–d) of the cortex. Yellow arrows in panel c show the fluorescence clusters, and white arrows show the contour of the labeled cells. All DCX signals are co-localized with NeuN, a mature neuron marker. Large differences in the distribution of DCX-positive cells were observed in the cortex of adjacent sections. Scale bars: 50 μm in A-a, A-b and A-d; 20 μm in A-c. (B) Emission wavelength and intensity of DCX immunofluorescence: The adjacent sections were double immunolabeled by the combination of DCX antibody (ab18723-1) and the fluorescent secondary antibody (A10036, Thermo Fisher Scientific) and the combination of NeuN antibody (ab104224) with secondary antibody (A11029), as red and green, respectively. In panel a, the low magnification image shows the localization of the detected neuron in the cerebral cortex (white frame), and the strong fluorescent point in the perikarya is indicated with the yellow arrow. Panels b and c respectively show the wavelength, intensity and localization of fluorescence in the tested points (color frames) on the pyramidal neuron immunolabeled by DCX (b') and NeuN (c') with an excitation wavelength of 579 nm (upper) or 495 nm. Panels b'' and c'' display the detected data of the emission wavelength and the fluorescence intensity for the different tested points. I–V: Different layers of the cerebral cortex. Scale bars: 200 μm in panel B-a and 50 μm in panels B-b' and B-c'. CST: Cell Signaling Technology; DCX: doublecortin.
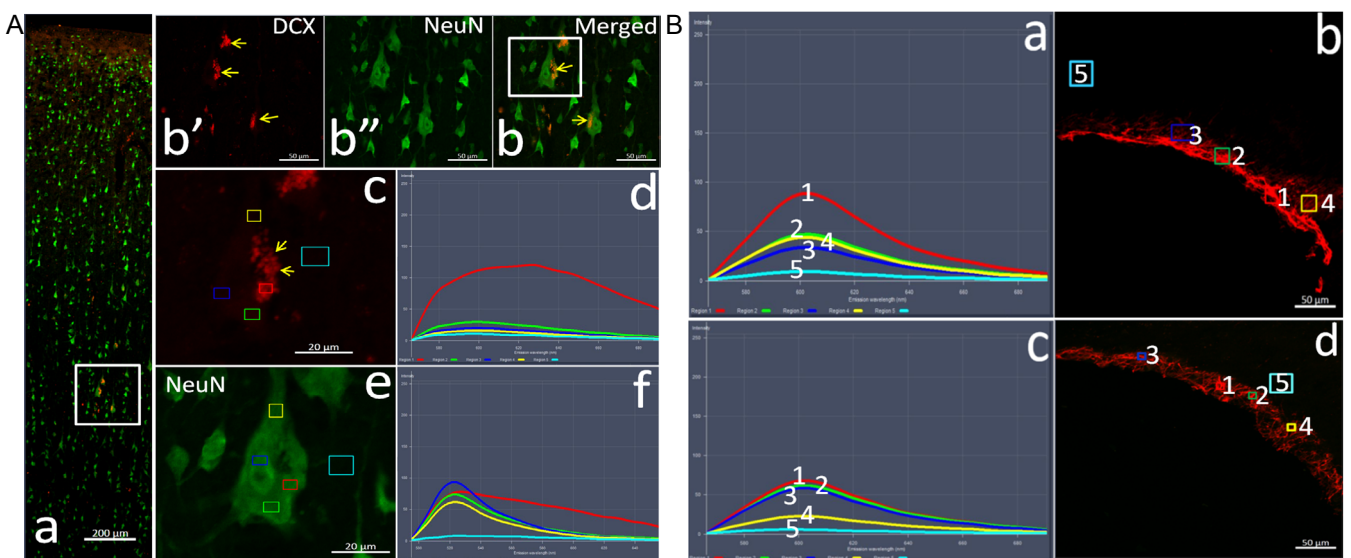

Figure 2 Changes in DCX labeling and emission spectra of the adjacent sections after antibody tissue adsorption.
(A) Staining and spectral pattern in the cerebral neocortex. The adjacent sections from the cortex and subventricular zone of the adult macaque were immunolabeled with the tissue-adsorbed DCX antibody (Ab18723-1) and fluorescein-conjugated secondary antibody (11036, Thermo Fisher Scientific) (red). NeuN is labeled green. In panels A-a, the low magnification pictures of the cortex show its hierarchical structure. Panels A-b'-b are the high magnification images of the region in the white frame in panel a, showing the DCX-positive neurons and the localization of the autofluorescent clusters (yellow arrows) with NeuN in the perikaryon. Images A-c and e are higher magnifications of the region in the white box in panel A-b, and color boxes represent the test sites of the spectrum. Panels A-d and f are the emission spectra taken from different sites (color frames) on the perikarya and background of images respectively, for excitation wavelengths of 561 nm (A-c and -d) and 488 nm (A-e and -f). Scale bars: 200 μm in panel A-a, 50 μm in A-b, and 20 μm in panels A-c and -e. (B) Changes in DCX labeling and the emission spectra after tissue adsorption in the subventricular zone. Panels show the emission spectra from the subventricular zone using unadsorbed (a and b) and tissue-adsorbed (c and d) antibodies for an excitation wavelength of 561 nm. Numbers in B-a and B-c correspond to those in graphs B-b and B-d, respectively. Scale bars: 50 μm in B-b and -d. DCX: Doublecortin; Lv: lateral ventricles.

Discussion

Comparative distribution of DCX-positive cells in adjacent sections of cortex and SVZ reveals the presence of antibody cross reactivity

Five DCX antibodies from different companies were used in our experiments for immunohistochemistry of adjacent sections of the neocortex and the SVZ of the adult primate (Kriegstein and Alvarez-Buylla, 2009; Kelsch et al., 2010). Their abilities to recognize DCX proteins have been confirmed by their identical staining of the SVZ. Therefore, the differences in labeling among the different DCX antibodies in adjacent cortex sections indicate non-specificity of some of these antibodies. The differential cortical DCX staining obtained with different batches of the polyclonal antibodies ab18723-1 (Lot. GR281032-1) and ab18723-2 (Lot. GR3224908-1) is another example of antibody cross reactivity.

Although in western blot assay, the different antibodies all successfully detected DCX at the predicted molecular weight, their specificity varied when the whole membrane was used in imaging development. Some high molecular weight bands detected by one DCX antibody (Abcam) appear to be non-specific. The molecular weights of these extraneous bands differ between antibody batches but remain consistent across tissues and experimental conditions. In addition, the degree of non-specificity seems to vary among species. Only a weak non-specific band appears in western blot assay using brain tissues from P0 rat. Given the large difference in DCX expression between newborn rats and adult monkeys, attention should be paid to the non-specificity of DCX in the macaque. It is worth noting that these antibodies have been validated by western blot assay and immunohistochemistry by the antibody company in these two species. The unexpected non-specificity might be the result of inadequate optimization of antibodies for different species in antibody production.

Antibody adsorption experiments confirm the presence of antibody cross reactivity

To further confirm the cross reactivity in the cortex sections, tissue adsorption and antigen neutralization experiments were performed. As the DCX protein sequence used for antibody preparation is highly conserved across species, we chose rat cortex to conduct tissue adsorption. Because the structure of the parietal cortex of the rat brain is relatively flat without any sulcus or gyrus, it is easily separated from the subcortical structures, thereby avoiding the potential impact of neurogenesis. Another reason for using rat cortex is their low non-specificity based on the result of western blot assay. DCX-positive labeling disappeared in cortical neurons but remained in the SVZ, demonstrating that the antibodies contained components that reacted with cortical tissues.

When using pre-adsorbed antibody Ab18723-1 and 2 for western blot, the predicted DCX band (40–45 kDa) disappeared in every lane, while the non-specific band was attenuated but not completely eliminated. This indicates that DCX is expressed in adult rat and monkey cortex, but at extremely low levels. Indeed, we failed to find any DCX-positive cell in monkey cortex during the whole experiment. The non-specific band could not be completely blocked by pre-adsorption, suggesting that the non-specificity varies among species.

There was no DCX-positive labeling in the SVZ sections labeled by DCX antibodies ab18723-1 and ab18723-2 that had been pre-incubated with DCX antigen, suggesting that the antibodies against DCX had been completely bound by DCX antigen. However, while the intensity of the fluorescence in the cortex decreased significantly, it remained visible. Although the fluorescence intensity in the cortex was reduced further when tissue pre-adsorbed secondary antibodies were used, the DCX signal was still distinguishable from background. These results suggest the presence of three types of IgG in the DCX antibodies: (1) Specific IgG binding only DCX, (2) IgG binding to DCX as well as some component of cortical neurons, and (3) IgG binding only to cortex neurons by cross-reaction even after antigen neutralization.

Other factors affecting the immunofluorescence results

In DCX antibody omission experiments, weak fluorescence still appeared in a few cortical neurons, and become weaker or even disappeared when tissue pre-adsorped secondary antibodies were used. This indicates the presence of non-specific reactivity in the Alexa Fluor-conjugated secondary antibodies that could result in staining artefacts.

Tissue autofluorescence is common in biological observations, and many factors can contribute to this phenomenon (Barnes et al., 2011; Reinert et al., 2011). In the current study, autofluorescence was demonstrated by the following evidence: (1) Fluorescent clusters were present in the sections with or without antibody treatment, especially in sections that were directly mounted after cutting; (2) The emission wavelength of the fluorescent cluster was far beyond the range of fluorescein emission wavelength; and (3) The mass's fluorescence was not easily quenched by laser under the confocal microscope. It is likely that this autofluorescence could be mistaken for DCX immunofluorescence, and therefore may confound the study of neurogenesis in the cerebral cortex.

Interpretation of previous investigations of the DCX-positive cells in the adult primate cerebral cortex

When reviewing previous reports on neurogenesis in the neocortex, we were astonished to learn that the distribution of DCX-positive immature neurons in the adult neocortex of primates varied greatly among the papers, which prompted us to take a closer look at the experimental methods used. Most previous studies on DCX-positive immature neurons in the adult cortex were based on immunoenzymatic methods (Qin et al., 2000; Cai et al., 2009; Zhang et al., 2009; Bloch et al., 2011; Fasemore et al., 2018). However, excessive development of the enzyme reaction may strengthen the original weak immunolabeling caused by cross-reactivity of antibodies, resulting in signal artefact. Indeed, in some reports, almost all the neurons, including pyramidal cells in the cerebral cortex, of adult primates were labeled by DCX antibody (Qin et al., 2000; Bloch et al., 2011). The situation might be improved with slice pre-treatment with NaBH4

for enhanced specificity and intensity of the signal (Moreno-Jimenez et al., 2019). Furthermore, the specificities of primary and secondary antibodies should be investigated in advance, as potential non-specificity and cross reactivity with tissues and other applied antibodies are a rather common phenomenon, especially for polyclonal antibodies (Harris et al., 1997; Craig et al., 1998). One should also be aware of spontaneous autofluorescence in the cortex. The impact of these potential artefacts should be taken into consideration and eliminated by setting up multiple control groups.

In addition to DCX, a marker of postmitotic neuronal progenitor cells and early immature neurons (Brown et al., 2003; Ehninger and Kempermann, 2008), various other biomarkers are specifically expressed during adult neuronal proliferation. These include the neural cell adhesion molecule PSA-NCAM and the neuronal determination protein NeuroD, both of which are usually expressed in the late phase of neurogenesis (Seki, 2002a, b; von Bohlen und Halbach, 2011). In our study, DCX was chosen because of its continuous expression during the intermediate progenitor cell stages, as it is expressed in type-2a, 2b and type 3 cells (Brandt et al., 2003; Brown et al., 2003; Filippov et al., 2003). The various stages of neurogenesis can be studied using a combination of these markers.

In summary, the putative DCX-positive neurons in the adult primate neocortex detected by immunofluorescence are likely artefacts caused by cross reactivity of the DCX primary antibodies, non-specific labeling by secondary antibodies or autofluorescence. DCX expression in the adult mammalian cortex might be much lower than previously reported.

Additional files:
Additional Figure 1: Schematic map of different cortical areas chosen for the localization of series sections.
Additional Figure 2: Graphic illustration of tissue adsorption procedures.
Additional Figure 3: DCX positive labeling in the adjacent sections of cerebral cortex of adult monkey.
Additional Figure 4: Omitting experiment of DCX primary antibody.
Additional Table 1: The primary and secondary antibodies used in the study.
Additional Table 2: Omitting experiment of DCX primary antibody.

References

Abrous DN, Koehl M, Le Moal M (2005) Adult neurogenesis: from precursors to network and physiology. Physiol Rev 85:523-569.

Barnes JA, Ebner BA, Duvick LA, Gao W, Chen G, Orr HT, Ebner TJ (2011) Abnormalities in the climbing fiber-Purkinje cell circuitry contribute to neuronal dysfunction in ATXN1[82Q] mice. J Neurosci 31:12778-12789.

Bloch J, Kaeser M, Sadeghi Y, Rouiller EM, Redmond DE Jr., Brunet JF (2011) Doublecortin-positive cells in the adult primate cerebral cortex and possible role in brain plasticity and development. J Comp Neurol 519:775-789.

Boldrini M, Fulmore CA, Tartt AN, Simeon LR, Pavlova I, Poposka V, Rosoklija GB, Stankov A, Arango V, Dwork AJ, Hen R, Mann JJ (2018) Human hippocampal neurogenesis persists throughout aging. Cell Stem Cell 22:589-599.

Bonfanti L, Nacher J (2012) New scenarios for neuronal structural plasticity in non-neurogenic brain parenchyma: the case of cortical layer II immature neurons. Prog Neurobiol 98:1-15.

Brandt MD, Jessberger S, Steiner B, Kronenberg G, Reuter K, Bick-Sander A, von der Behrens W, Kempermann G (2003) Transient calretinin expression defines early postmitotic step of neuronal differentiation in adult hippocampal neurogenesis of mice. Mol Cell Neurosci 24:603-613.

Brown JP, Couillard-Despres S, Cooper-Kuhn CM, Winkler J, Aigner L, Kuhn HG (2003) Transient expression of doublecortin during adult neurogenesis. J Comp Neurol 467:1-10.

Cai Y, Xiong K, Chu Y, Luo DW, Luo XG, Yuan XY, Struble RG, Clough RW, Spencer DD, Williamson A, Kordower JH, Patrylo PR, Yan XX (2009) Doublecortin expression in adult cat and primate cerebral cortex relates to immature neurons that develop into GABAergic subgroups. Exp Neurol 216:342-356.

Craig L, Sanschagrin PC, Rozek A, Lackie S, Kuhn LA, Scott JK (1998) The role of structure in antibody cross-reactivity between peptides and folded proteins. J Mol Biol 281:183-201.

Dhaliwal J, Xi Y, Bruel-Jungerman E, Germain J, Francis F, Lagace DC (2015) Doublecortin (DCX) is not essential for survival and differentiation of newborn neurons in the adult mouse dentate gyrus. Front Neurosci 9:494.

Diem K, Magaret A, Klock A, Jin L, Zhu J, Corey L (2015) Image analysis for accurately counting CD4+ and CD8+ T cells in human tissue. J Virol Methods 222:117-121.

Drury JA, Nik H, van Oppenraaij RH, Tang AW, Turner MA, Quenby S (2011) Endometrial cell counts in recurrent miscarriage: a comparison of counting methods. Histopathology 59:1156-1162.

Ehninger D, Kempermann G (2008) Neurogenesis in the adult hippocampus. Cell Tissue Res 331:243-250.

Fasemore TM, Patzke N, Kaswera-Kyamakya C, Gilissen E, Manger PR, Ihunwo AO (2018) The distribution of Ki-67 and doublecortin-immunopositive cells in the brains of three strepsirrhine primates: galago demidoff, perodicticus potto, and lemur catta. Neuroscience 372:46-57.

Feliciano DM, Bordey A, Bonfanti L (2015) Noncanonical sites of adult neurogenesis in the mammalian brain. Cold Spring Harb Perspect Biol 7:a018846.

Filippov V, Kronenberg G, Pivneva T, Reuter K, Steiner B, Wang LP, Yamaguchi M, Kettenmann H, Kempermann G (2003) Subpopulation of nestin-expressing progenitor cells in the adult murine hippocampus shows electrophysiological and morphological characteristics of astrocytes. Mol Cell Neurosci 23:373-382.

Fournier J, Muller CM, Schneider I, Laurent G (2018) Spatial information in a non-retinotopic visual cortex. Neuron 97:164-180 e167.

Fung SJ, Joshi D, Allen KM, Sivagnanasundaram S, Rothmond DA, Saunders R, Noble PL, Webster MJ, Weickert CS (2011) Developmental patterns of doublecortin expression and white matter neuron density in the postnatal primate prefrontal cortex and schizophrenia. PLoS One 6:e25194.

Gould E, Reeves AJ, Graziano MS, Gross CG (1999) Neurogenesis in the neocortex of adult primates. Science 286:548-552.

Han J, Zhang JZ, Zhong ZF, Li ZF, Pang WS, Hu J, Chen LD (2018) Gualou Guizhi decoction promotes neurological functional recovery and neurogenesis following focal cerebral ischemia/reperfusion. Neural Regen Res 13:1408-1416.

Harris SL, Craig L, Mehroke JS, Rashed M, Zwick MB, Kenar K, Toone EJ, Greenspan N, Auzanneau FI, Marino-Albernas JR, Pinto BM, Scott JK (1997) Exploring the basis of peptide-carbohydrate crossreactivity: evidence for discrimination by peptides between closely related anti-carbohydrate antibodies. Proc Natl Acad Sci U S A 94:2454-2459.
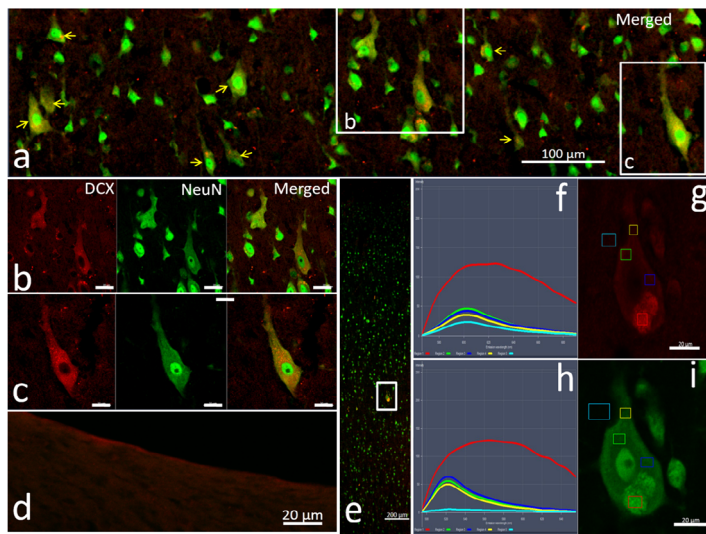
Figure 3 Antigen adsorption of DCX antibodies.
Antibody combination of the antigen-adsorbed DCX antibody ab18723-1 and the secondary antibody ab150072 (unadsorbed) was first used to label the adjacent sections of the cortex and subventricular zone. Panel a is taken from the fifth layer of the cortex (Additional Figure 4) to show the NeuN/DCX double-labeled neurons (yellow arrows). In b and c image series from the white boxes in panel a, DCX immunoreactivity (red) was reduced after adsorption, but medium intensity red fluorescence persisted. Panel d shows no DCX-positive labeling in the subventricular zone after the DCX antibody was adsorbed by DCX antigen. To distinguish the source of red fluorescence that remains after DCX antibody adsorption, the adjacent sections of adult macaque cortex were immunolabeled with the antigen-adsorbed DCX antibody (ab18723-1) and the secondary antibody (ab150072) that had been pre-adsorbed with a rat cortex section. Panel e shows the localization of the tested neuron in the cortex (white box). Panels f and h show the spectral features of the images in g and i, respectively. In graph g and i, small boxes in different colors represent the locations of spectral analysis spots. Red: Autofluorescence; green, blue and yellow represent immunofluorescence from the tested sites; light blue: the background. In these sections labeled by antigen pre-adsorbed DCX antibody, the immunofluorescence intensity of some neurons is still higher than the background, indicating the presence of cross reactivity. Scale bars: 200 μm in panel e, 100 μm in panel a, and 20 μm in panels b–d, g and i. DCX: Doublecortin; Lv: lateral ventricle.
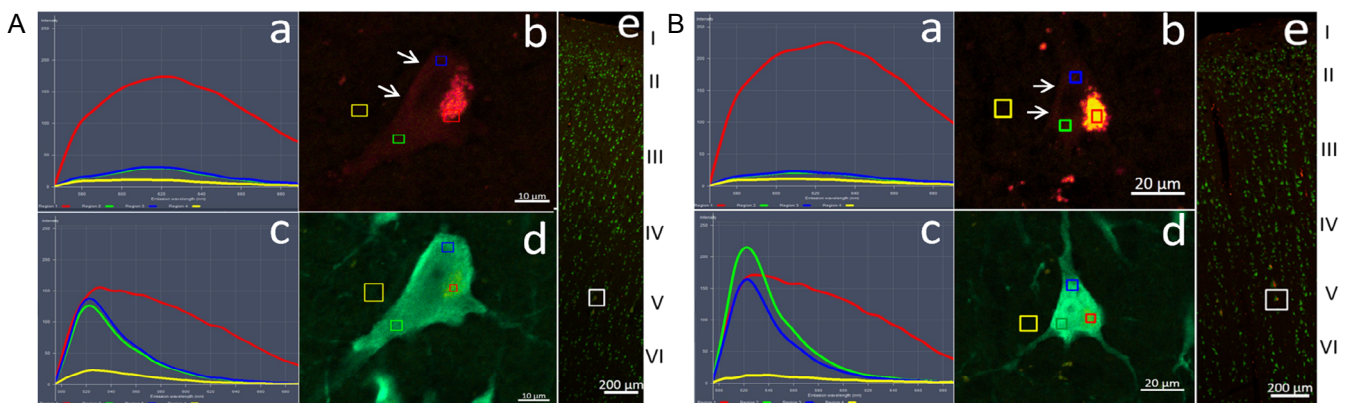

Figure 4 Non-specific staining demonstrated by DCX primary omission experiment with unadsorbed or adsorbed secondary antibodies.
The sections were incubated with NeuN antibody and secondary antibodies A10029 (green, corresponding to NeuN) and ab150072 (red, Abcam) without (A) or with (B) tissue adsorption. Panels a and c in A and B are the spectral profiles for excitation wavelengths of 561 nm (upper) and 488 nm (lower). Panels b and d are the high magnification images of the white frames in the low magnification images of the cortex (panel e), indicating the test sites of the corresponding spectrograms in panels a and c of A and B. The white arrows in b of A and B indicate the contour of the neurons labeled by secondary ab150072 only. The color curves in A-a and c and B-a and c correspond to the color frames in panel A-b and d, B-b and d. Red curve: Spontaneous autofluorescence; green and blue: non-specific labeling by secondary antibody; yellow curve: background fluorescence. Scale bars: 10 μm in A-b and d, 20 μm in B-b and d, and 200 μm in A-e and B-e. DCX: Doublecortin.

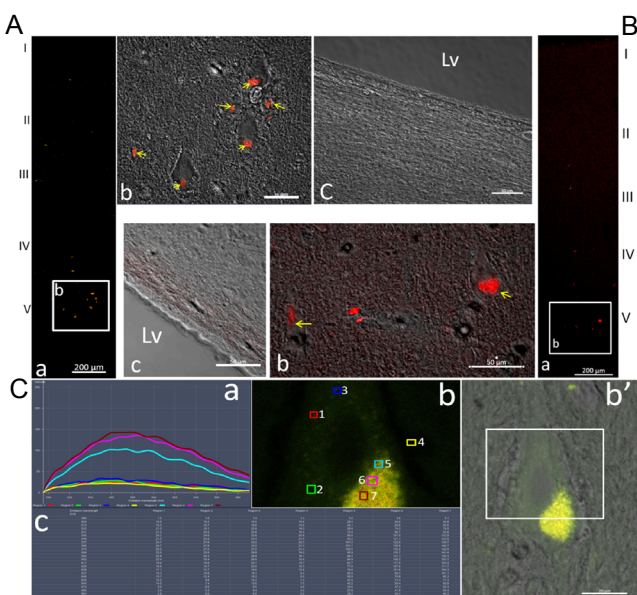**Figure 5 Autofluorescence in neurons of the cerebral cortex of the adult macaque.**
(A) Adjacent cryostat sections of the adult macaque cortex were mounted with a cover glass directly and immediately after slicing, without any other treatment (a–c, upper left). Panel A-a shows the localization of the autofluorescent particles in the low magnification image. Panel A-b is the merged high magnification image from confocal and phase contrast microscopy from the white frame in panel a, showing the localization of the autofluorescent particles (yellow arrows) in the neuron in lamina V. Panel A-c is the merged high magnification image from laser confocal and phase contrast microscopy of the subventricular zone, and no autofluorescent particles were found in this area. (B) Adjacent sections incubated with the serum diluents without any primary or secondary antibody (a–c, low upper). Panel a is the low magnification image of the cortex, showing the autofluorescent clusters and particles in the cortex. The merged high magnification image from laser confocal and phase contrast microscopy (b) is the magnified image of the white frame in panel a to show the localization of the autofluorescent particles (yellow arrows) within the neurons of lamina V. Panel c is another merged image of confocal and phase contrast images of the subventricular zone without any autofluorescence. Scale bars: 200 μm in panels A-a and B-a; 50 μm in panel A-b, -c and B-b, -c. (C) Autofluorescence intensity and emission wavelength of a pyramidal cell in layer V of the adult monkey cortex (a, b and b', c): The adjacent cryostat sections were mounted with a cover glass directly and immediately after slicing, without any other treatment. When excited at 488 nm, the wavelength and intensity (a and c) of the emission spectra of the fluorescence points (b) were measured using a laser scanning confocal microscope. Scale bars: 20 μm in C-b and -b'. The numbers next to the small boxes in different colors represent the location and order of the fluorescent dots. 1–3: The background fluorescence within the cytoplasm of the neuron; 4: background fluorescence; 5–7: fluorescence at different positions of the autofluorescent cluster. The color of the fluorescence corresponds to the color of the detection sites (boxes). (b') The merged images of the laser scanning confocal (autofluorescence) and phase contrast microscope. The tested region in the pyramidal neuron in layer V of the cortex is indicated in the white frame. (c) The intensity of the detected fluorescence wavelength of the different test points. Lv: Lateral ventricle.
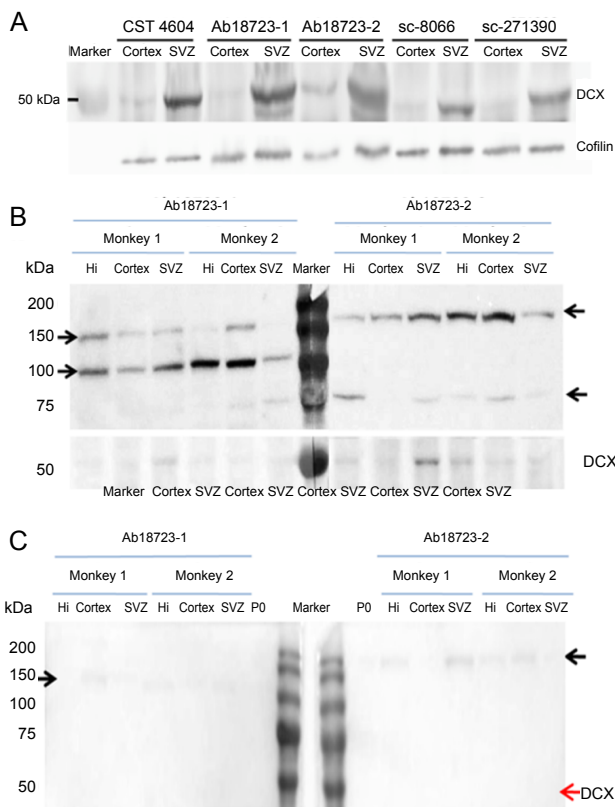
Figure 6 Comparison of western blot assays of the adult macaque brain using the various antibodies.

(A) Differences in western blot results among the various DCX antibodies. Either cortex or SVZ of the same monkey was lysed, and 25 μg of total protein was loaded per lane. Polyvinylidene fluoride membranes were incubated with different DCX antibodies and were aligned for image development. Cofilin was used as control. (B) Western blot showing the non-specificity of DCX antibodies. Different batches of Ab18723 were used to detect the target protein from monkeys. A total of 25 μg protein from the hippocampus, cortex and SVZ of rhesus macaques were loaded per lane. The blot was cut for antibody incubation and the strips were aligned before image development. Protein bands not mentioned in the antibody datasheet were observed in monkeys but not in rats. The molecular weight of those bands differed between batches. (C) The non-specific band could not be completely blocked by pre-adsorption. Tissue pre-adsorbed DCX antibodies Ab18723-1 and 2 were used to detect DCX in 6 μg total brain protein from P0 rat and 25 μg total protein from the hippocampus, cortex and SVZ of adult rhesus macaques. The predicted DCX band (40–45 kDa) disappears in every lane, while the non-specific band is attenuated but not completely eliminated. Arrows on either side indicate the molecular weights. CTS: Cell Signaling Technology; DCX: doublecortin; Hi: hippocampus; SVZ: subventricular zone.

He HW, Zhang YL, Yu BQ, Ye G, You W, So KF, Li X (2019) Soluble Nogo receptor 1 fusion protein protects neural progenitor cells in rats with ischemic stroke. Neural Regen Res 14:1755-1764.

Jensen EC (2013) Quantitative analysis of histological staining and fluorescence using ImageJ. Anat Rec (Hoboken) 296:378-381.

Kelsch W, Sim S, Lois C (2010) Watching synaptogenesis in the adult brain. Annu Rev Neurosci 33:131-149.

Kempermann G, Gage FH, Aigner L, Song H, Curtis MA, Thuret S, Kuhn HG, Jessberger S, Frankland PW, Cameron HA, Gould E, Hen R, Abrous DN, Toni N, Schinder AF, Zhao X, Lucassen PJ, Frisen J (2018) Human adult neurogenesis: evidence and remaining questions. Cell Stem Cell 23:25-30.

Kornack DR, Rakic P (2001) Cell proliferation without neurogenesis in adult primate neocortex. Science 294:2127-2130.

Kriegstein A, Alvarez-Buylla A (2009) The glial nature of embryonic and adult neural stem cells. Annu Rev Neurosci 32:149-184.

Lipp HP, Bonfanti L (2016) Adult neurogenesis in mammals: variations and confusions. Brain Behav Evol 87:205-221.

Liu JYW, Matarin M, Reeves C, McEvoy AW, Miserocchi A, Thompson P, Sisodiya SM, Thom M (2018) Doublecortin-expressing cell types in temporal lobe epilepsy. Acta Neuropathol Commun 6:60.

Liu YW, Curtis MA, Gibbons HM, Mee EW, Bergin PS, Teoh HH, Connor B, Dragunow M, Faull RL (2008) Doublecortin expression in the normal and epileptic adult human brain. Eur J Neurosci 28:2254-2265.

Model MA, Burkhardt JK (2001) A standard for calibration and shading correction of a fluorescence microscope. Cytometry 44:309-316.

Moreno-Jimenez EP, Flor-Garcia M, Terreros-Roncal J, Rabano A, Cafini F, Pallas-Bazarra N, Avila J, Llorens-Martin M (2019) Adult hippocampal neurogenesis is abundant in neurologically healthy subjects and drops sharply in patients with Alzheimer's disease. Nat Med 25:554-560.

Moslehi M, Ng DCH, Bogoyevitch MA (2017) Dynamic microtubule association of Doublecortin X (DCX) is regulated by its C-terminus. Sci Rep 7:5245.

Nacher J, Bonfanti L (2015) New neurons from old beliefs in the adult piriform cortex? A Commentary on: "Occurrence of new neurons in the piriform cortex". Front Neuroanat 9:62.

Piumatti M, Palazzo O, La Rosa C, Crociara P, Parolisi R, Luzzati F, Levy F, Bonfanti L (2018) Non-newly generated, "immature" neurons in the sheep brain are not restricted to cerebral cortex. J Neurosci 38:826-842.

Qin J, Mizuguchi M, Itoh M, Takashima S (2000) Immunohistochemical expression of doublecortin in the human cerebrum: comparison of normal development and neuronal migration disorders. Brain Res 863:225-232.

Rakic P (2002) Neurogenesis in adult primate neocortex: an evaluation of the evidence. Nat Rev Neurosci 3:65-71.

Reinert KC, Gao W, Chen G, Wang X, Peng YP, Ebner TJ (2011) Cellular and metabolic origins of flavoprotein autofluorescence in the cerebellar cortex in vivo. Cerebellum 10:585-599.

Schaar BT, Kinoshita K, McConnell SK (2004) Doublecortin microtubule affinity is regulated by a balance of kinase and phosphatase activity at the leading edge of migrating neurons. Neuron 41:203-213.

Schindelin J, Arganda-Carreras I, Frise E, Kaynig V, Longair M, Pietzsch T, Preibisch S, Rueden C, Saalfeld S, Schmid B, Tinevez JY, White DJ, Hartenstein V, Eliceiri K, Tomancak P, Cardona A (2012) Fiji: an open-source platform for biological-image analysis. Nat Methods 9:676-682.

Seki T (2002a) Hippocampal adult neurogenesis occurs in a microenvironment provided by PSA-NCAM-expressing immature neurons. J Neurosci Res 69:772-783.

Seki T (2002b) Expression patterns of immature neuronal markers PSA-NCAM, CRMP-4 and NeuroD in the hippocampus of young adult and aged rodents. J Neurosci Res 70:327-334.

Shahsavani M, Pronk RJ, Falk R, Lam M, Moslem M, Linker SB, Salma J, Day K, Schuster J, Anderlid BM, Dahl N, Gage FH, Falk A (2018) An in vitro model of lissencephaly: expanding the role of DCX during neurogenesis. Mol Psychiatry 23:1674-1684.

Stanton GB, Kohler SJ, Boklweski J, Cameron JL, Greenough WT (2015) Cytogenesis in the adult monkey motor cortex: perivascular NG2 cells are the major adult born cell type. J Comp Neurol 523:849-868.

Tobin MK, Musaraca K, Disouky A, Shetti A, Bheri A, Honer WG, Kim N, Dawe RJ, Bennett DA, Arfanakis K, Lazarov O (2019) Human hippocampal neurogenesis persists in aged adults and Alzheimer's disease patients. Cell Stem Cell 24:974-982.

Vayrynen JP, Vornanen JO, Sajanti S, Bohm JP, Tuomisto A, Makinen MJ (2012) An improved image analysis method for cell counting lends credibility to the prognostic significance of T cells in colorectal cancer. Virchows Arch 460:455-465.

von Bohlen und Halbach O (2011) Immunohistological markers for proliferative events, gliogenesis, and neurogenesis within the adult hippocampus. Cell Tissue Res 345:1-19.

Zhang XM, Cai Y, Chu Y, Chen EY, Feng JC, Luo XG, Xiong K, Struble RG, Clough RW, Patrylo PR, Kordower JH, Yan XX (2009) Doublecortin-expressing cells persist in the associative cerebral cortex and amygdala in aged nonhuman primates. Front Neuroanat 3:17.

Zhou WB, Miao ZN, Zhang B, Long W, Zheng FX, Kong J, Yu B (2019) Luteolin induces hippocampal neurogenesis in the Ts65Dn mouse model of Down syndrome. Neural Regen Res 14:613-620.
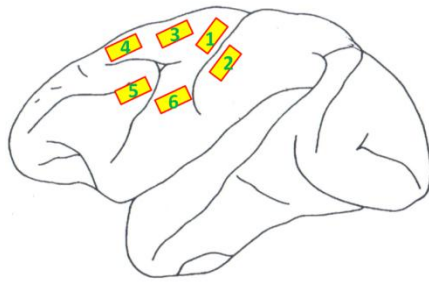
Additional Figure 1 Schematic map of different cortical areas chosen for the localization of series sections.
Tissues from the anterior central gyrus and the medial regions of the prefrontal cortex are collected to perform the experiment. The numbers (1-6) and the yellow frames represent different cortex areas.

DCX antibodies
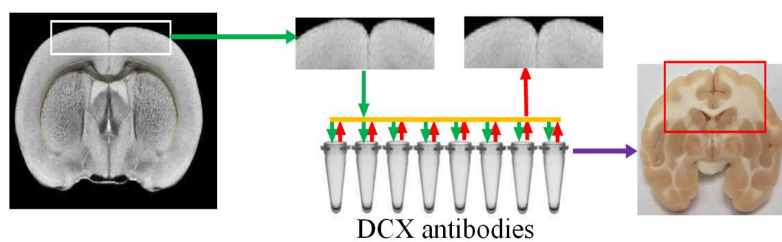
Additional Figure 2 Graphic illustration of tissue adsorption procedures.

The rat cortex sections (20 μm thickness, emphasized with white box without any non-cortical components) were cut and permeabilized with Triton for two hours, they were then added to the antibodies at their working dilutions for 6 hours at 4 °C. After the first incubation, tissues was changed and the absorbing process was repeated once more. The sections that were fished out from the absorbing antibodies were incubated with corresponding fluorescein conjugated secondary antibodies to detect the adsorption effect. The adsorped antibodies were later used in the incubation with cortex and SVZ of monkey tissues (red box).
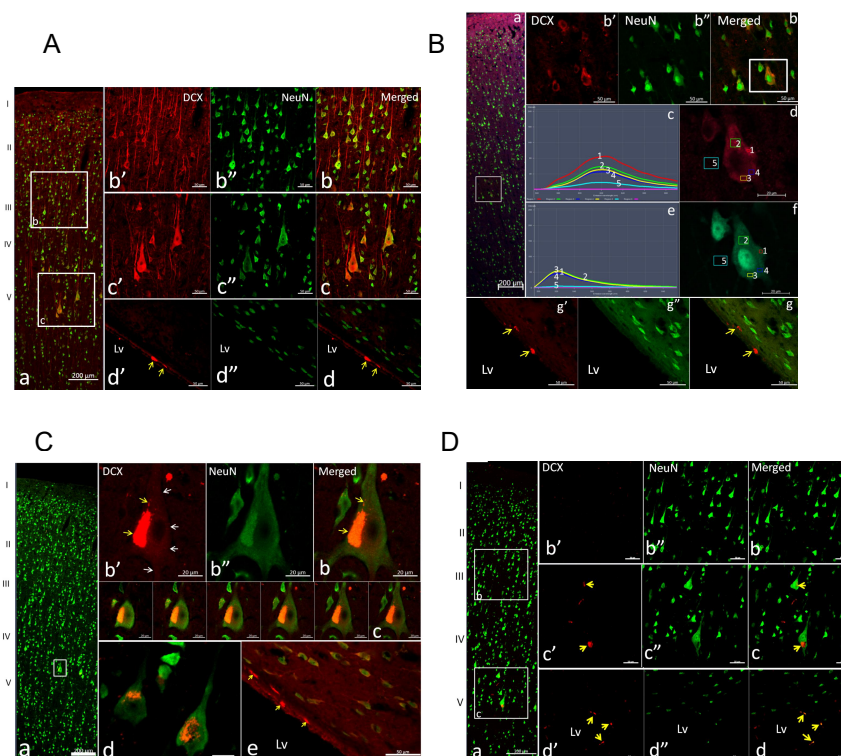
Additional Figure 3 DCX positive labeling in the adjacent sections of cerebral cortex of adult monkey.
(A) Staining combination: DCX (Ab18723-1) with Ab150072. The section of the cerebral cortex of the adult macaque was double immunolabeled with two kinds of antibodies, DCX (Ab18723-1) and NeuN (ab104224) and the corresponding secondary antibodies, Ab150072 and Themo A1102 as red and green, respectively. Panels b and c, the magnification images of the white frames in panel a to show DCX positive labeling and the localization in the NeuN positive neuron. Panels d'-d show DCX positive labeling (yellow arrows) in the SVZ. Lv, lateral ventricle. I to V, different layers of the cerebral cortex. Scale bars: 200 μm in Panel a, 50 μm in Panel b and d. (B) Staining combination: DCX (Ab18723-2) with Ab150072. The crystal sections of the cerebral cortex of the adult monkey were labeled with DCX (Ab18723-2) and NeuN primary antibody, combined with fluorescein conjugated secondary antibodies (ab150072 and Thermo A10029). The confocal images were taken using the same photograph conditions. Panel a, the low magnification image and panel b'-b, d and f are a series of magnified images of the white frames in the panel a and b, showing the DCX positive labeling and their co-localization with NeuN. Numbers on curves in panel c and e represent the wavelength and intensity of fluorescence in the detected regions on images d and f (Frames with different color). Panels g'-g show DCX positive labelings (yellow arrows) in SVZ. Lv, lateral ventricles. Sclae bars: 200 μm in panel a, 50 μm in panel b-b' and g'-g, 20 μm in panel d and f. (C) Staining combination: DCX (CST#4604) with Ab150072. The crystal sections of the cerebral cortex of the adult monkey were labeled with DCX (CST#4604) and NeuN primary antibody, combined with fluorescein conjugated secondary antibodies (ab150072 and Thermo A10029). Panel a, stitching image at low magnification. Panel b'-b, high magnified images of the white frame in panel a, showing the weak (white arrows) and strong red fluorescence (yellow arrows) and their co-localization with NeuN staining. Panel C, series layered scanning images, step=1 μm. Panel d, another merged images showing the relationship of red fluorescence clumps and NeuN positive pericaryon. Panel e, SVZ is only labeled by DCX immunolabeling (yellow arrows), rather than NeuN. Lv, lateral ventricle. Sclae bars: 200 μm in panel a, 50 μm in e, and 20 μm in b to d. (D) Staining combination: DCX (SC-271390) with A10031. The crystal sections of the cerebral cortex of the adult monkey were labeled with DCX primary antibody (SC-271390) and fluorescein conjugated secondary antibody (Thermo A10031) and NeuN. The confocal images were taken using the same photograph conditions. Panel a, the low magnification image, panel b'-b and c'-c, magnified images of the white frames in panel a, showing the fluorescence clumps (yellow arrows) and their co-localization in the NeuN+ neuron. Panel d'-d was taken from the SVZ to show DCX labeling (yellow arrow). Lv, lateral ventricle. Sclae bars: 200 μm in panel a, 50 μm in panel b-d. DCX: Doublecortin X.
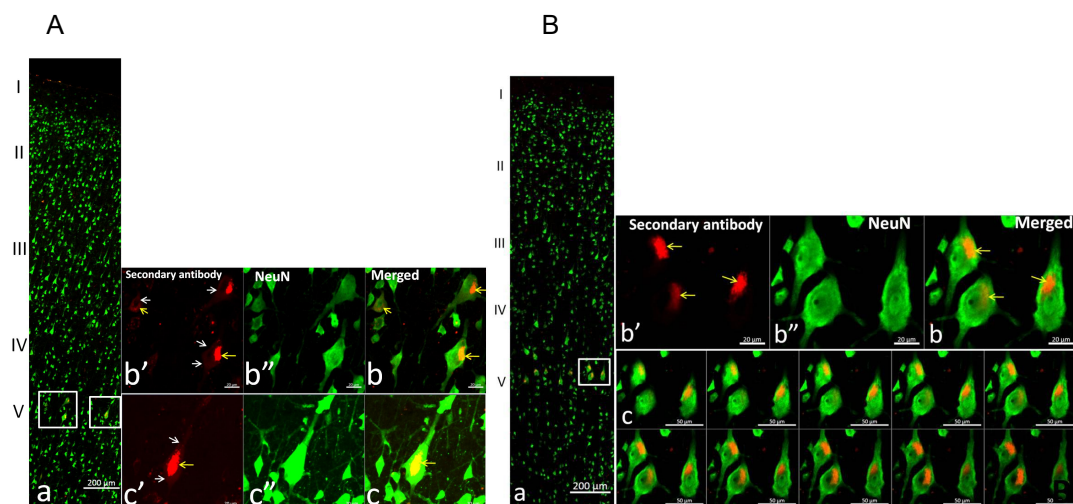
Additional Figure 4 Omitting experiment of DCX primary antibody.
(A) DCX Primary omitting experiment with secondary antibody applied. To demonstrate non-specific labelings caused by secondary antibody, DCX primary antibody omitting experiments were implemented. The cerebral cortex sections of the adult macaque were incubated with primary antibody NeuN and secondary antibodies ab150072 (red, abcam) and A10029 (green, Thermo, corresponding to NeuN antibody). Panel a is a low magnification photograph, and panels b and c are the high magnification images of white frames in the panel a. The results show not only the intense spontaneous red fluorescence (yellow arrows), but also the red outline of the labeled pericaryons and their co-localization with NeuN in the pyramidal neurons (white arrows in b' and c'). Scale bars: 200 μm in panel a and 20 μm in panels b and c. (B) DCX Primary omitting experiment with pre-absorbed secondary antibody applied. To test whether the non-specific labelings exist in the secondary antibodies, nine kinds of secondary antibodies were pre-absorbed with the rat cortex sections. The adjacent sections of the cerebral cortex of the adult macaque were labeled with NeuN antibody and secondary antibodies ab150072 (red, Abcam, pre-absorbed by rat cortex sections) and A10029 (green, Thermo, corresponding to NeuN antibody). Panel a, the low magnification photograph, and panel b, the high magnification images of white frames in the panel a, shows the localization of the red autofluorescence lumps (yellow arrows) within NeuN positive pericaryon in the lamina V. Panel c, series of layered photographs (0.5μm/step×10) verifying that the red autofluorescence lumps are localized within the NeuN positive pericaryon of the pyramidal neuron rather than overlapping together. No red immunofluorescence exists in the pericaryon. Scale bars: 200 μm in panel a, 20 μm in panel b and 50 μm in panel c. DCX: Doublecortin X.

Additional Table 1 The primary and secondary antibodies used in the study

Antibodies	Antigens/peptides	Species	Producers	Identifiers	Fluorescein and Wavelength		
					Alexa Fluor	Excitation	Emission
DCX	YLPLSLDDSDSLGDSM	Rabbit (polyclone)	Abcam, MA, USA	Ab18723-1*			
DCX	YLPLSLDDSDSLGDSM	Rabbit (polyclone)	Abcam, MA, USA	Ab18723-2*			
DCX	"Epitope is centered around Leu349 and Tyr350 of the DCX"**	Rabbit (polyclone)	CST, MA, USA	CST#4604			
DCX	DLYLPLSLDDSDSLGDSM	Mouse (monoclone)	Santa Crus，TX, USA	SC-271390			
DCX	DLYLPLSLDDSDSLGDSM	Goat (polyclone)	Santa Crus，TX, USA	SC-8066			
NeuN	MAQPYPPAQYPPPPQNGIPAEYA PPPPHPTQDYSGQTPVPTEHGMT LYTPAQTHPEQPGSEASTQPIAG TQTVPQTDEAAQTDSQPLHPSDP TEKQQPKR	Mouse (monoclone)	Abcam, MA, USA	ab104224			
Anti-Goat	FC-of Goat lgG	Donkey	Abcam, MA, USA	Ab150131	647	652	668
Anti-mouse	FC-of mouse IgG	Donkey	Abcam, MA, USA	Ab150112	594	590	617
Anti-mouse	FC-of mouse lgG	Donkey	Abcam, MA, USA	Ab181289	488	495	519
Anti-rabbit	FC-of rabbit lgG	Donkey	Abcam, MA, USA	Ab150072	594	590	617
Anti-rabbit	FC-of rabbit lgG	Donkey	Abcam, MA, USA	Ab181346	488	495	519
Anti-mouse	FC-of mouse lgG	Goat	Thermo, MA, USA	A11029	488	495	519
Anti-mouse	FC-of mouse lgG	Goat	Thermo, MA, USA	A11031	568	579	606
Anti-rabbit	FC-of rabbit lgG	Goat	Thermo, MA, USA	A11034	488	495	519
Anti-rabbit	FC-of rabbit lgG	Goat	Thermo, MA, USA	A11036	568	579	606

* indicates different batches of antibodies under the same product number: Ab18723-1 (Lot.GR281032-1) and Ab18723-2 (Lot. GR3224908-1).** provided by CST company.
DCX: Human doublecortin.

Additional Table 2 Omitting experiment of DCX primary antibody

Brain region / Secondary antibodies	Cortex	SVZ
Abcam150112, unabsorbed/absorbed	+/±	±/±
Abcam150131, unabsorbed/absorbed	+/±	±/±
Abcam181289, unabsorbed/absorbed	±/±	±/±
Abcam150072, unabsorbed/absorbed	+/±	±/±
Abcam181346, unabsorbed/absorbed	±/±	±/±
Thermo A11029, unabsorbed/absorbed	±/±	±/±
Thermo A11031, unabsorbed/absorbed	±/±	±/±
Thermo A11034, unabsorbed/absorbed	±/±	±/±
Thermo A11036, unabsorbed/absorbed	±/±	±/±

"+", weak fluorescence. "±", weak immunofluorescence is only slightly higher than the background fluorescence in the subsequent quantitative spectroscopy examinations.

DCX: Doublecortin X.